Hyperbranched Blue to Red Light-Emitting Polymers with Tetraarylsilyl Cores: Synthesis, Optical and Electroluminescence Properties, and ab Initio Modeling Studies

Xue-Ming Liu, Tingting Lin, Junchao Huang, Xiao-Tao Hao, Kian Soo Ong, and Chaobin He*

Institute of Materials Research and Engineering, 3 Research Link, Singapore 117602

Received November 10, 2004; Revised Manuscript Received March 10, 2005

ABSTRACT: A series of hyperbranched alternating copolymers were synthesized by either Suzuki or Grignard coupling polycondensation reactions between two AB_4-type tetrahedral monomers [tetra(4-bromobiphenyl)silane (**1**) and tetra(2-bromo-9,9-dihexylfluorenyl)silane (**2**)] with AB_2-type dibromo or diboronic acid monomers of 9,9-dihexylfluorene or oligothiophenes. Polymers (**3**, **5**−**8**) (derived from **1** and 9,9-dihexylfluorene-2,7-diboronic acid, 2,2′-bithiophene-5,5′-diboronic acid, 2,2′:5′,2″-terthiophene-5,5″-diboronic acid, 5,5′-dibromo-3,3′-dihexyl-2,2′-bithiophene, and 5,5″-dibromo-3,3′-dihexyl-2,2′:5′,2″-terthiophene, respectively) emitted blue to red light in the solid state and their absorption and emission maxima were red shifted with the increase in conjugation length. Polymer **4** (derived from **2** and 9,9-dihexylfluorene-2,7-diboronic acid) emitted blue light highly efficiently in both solution and the condensed state, but its absorption and emission maxima were slightly blue-shifted from those of **3**, revealing that no effective electron delocalization occurred among the fluorene units. Polymer **9** (derived from **2** and 5,5′-dibromo-3,3′-dihexyl-2,2′-bithiophene) emitted intense blue light in solution with only the structured peaks from the fluorene units being observed in its PL spectra. The film of **9** emitted green light and emissions from both the fluorene and bithiophene chromophores were observed in the PL spectra with the latter being stronger, due to the intramolecular energy transfer from fluorene units to bithiophene units. The ab initio studies were carried out to elucidate the intrigue optical properties of the present hyperbranched polymers. Double layer devices with configurations ITO/PEDOT/polymer (**4** or **7**)/LiF/Ca/Ag, which emitted blue and green light, respectively, were fabricated and preliminary data on the device performances are reported. We present two strategies for the design and synthesis of RGB-emitting hyperbarched polymers: (1) using a structurally not crowded core **1** and adjusting the emission by conjugation length; (2) using a structurally crowded core **2** and adjusting the light emission by intramolecular energy transfer.

Introduction

9,9-Disubstituted fluorene-containing polymers and oligomers (PFs) have proven to be the most promising blue-light-emitting materials due to their excellent thermal and chemical stability and high PL efficiency.[1] Introduction of substitutes at C-9 of fluorene serves to increase solubility of PFs in organic solvents and block the reactive carbon site. Recently, full RGB emissions have been achieved by incorporating into wide band-gap PF backbones with narrow band-gap units, such as oligothiophenes[2] and benzothiadiazole.[3] In such heteropolymers, the narrow band-gap fluorophores function as an exciton trap, which allows efficient intramolecular energy transfer from the fluorene units to the narrow band-gap units to occur and hence realize green to red emissions.[4] A thorny problem associated with PFs is their tendencies of forming aggregates, excimers or ketone defects during either annealing or passage of current, which lead to red-shifted and less efficient emission and reduced color purity.[5] The ketone defects-related problems are caused by the presence of small amounts of fluorenones, which are resulted from oxidation of incompletely substituted species of fluorene and can be effectively reduced by monomer purification.[6] Many studies have been carried out to solve the aggregation-related problems by increasing the structural hindrances of PFs, thus reducing their self-aggregation tendency in the solid state. For example, studies on PFs containing bulky and oxidant-resistant groups at the 9-position,[7] cross-linked oligofluorene networks,[8] spirofluorene derivatives,[9] star-shaped,[10] ladder-type polyfluorenes,[11] and hyperbranched light-emitting polymers[12] have been reported.

Recently, structurally "awkward"[13] tetrahedral organic materials derived from several core compounds such as tetraphenylmethane[14] and tetraphenylsilane[15] have attracted much attention in the areas of chemistry and material sciences.[16−18] The tetrahedral approach has proven to be an effective method for designing nonaggregating amorphous optoelectronic materials.[19] We were interested in luminescent materials comprising several tetraarylmethane/silane tetrahedral cores and an oligosilsequioxane (POSS) octahedral core.[20] We have recently reported a novel class of hyperbranched blue-light-emitting alternating copolymers of tetrabromoarylmethane/silane and 9,9-dihexylfluorene-2,7-diboronic acid. We found that these nonaggregating polymers were highly efficient blue light emitters.[21] In a continuation of our research on tetrahedral luminescent materials, we herein report the synthesis, optical and electroluminescence properties of a series of hyperbranched alternating copolymers that were readily synthesized by either Suzuki or Grignard coupling polycondensation reactions between two AB_4-type tetrabromo monomers [tetra(4-bromobiphenyl)silane (**1**)

* Corresponding author. Fax: 65-68727528, E-mail: cb-he@imre.a-star.edu.sg.

10.1021/ma047686q CCC: $30.25
Published on Web 04/16/2005

Chart 1. Schematic Presentation of the Structures of the Hyperbranched Polymers

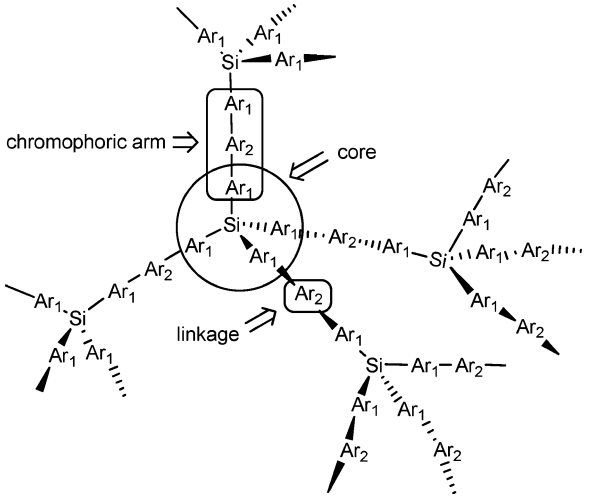

and tetra(2-bromo-9,9-dihexylfluorenyl)silane (**2**)] with AB_2-type dibromo/diboronic acid monomers of 9,9-dihexylfluorene or oligothiophenes. A schematic presentation of the general structure of these polymers is present in Chart 1. The structures of these polymers are composed of two parts: *tetrahedral cores* (from **1** or **2**) and *linkage units* (from AB_2 monomers) with repeating *chromophoric arms* ($Ar_1-Ar_2-Ar_1$) from both parts. By comparing the optical properties of analogue polymers derived from **1** and **2**, we found that (1) effective electron delocalization is present in the chromophoric arm of polymers derived from **1** and light-emission could be adjusted by controlling the conjugation length; (2) the hindered structure of **2** made electron-delocalization in the chromophoric arm of polymers derived from **2** not effective and consequently intramolecular energy transfer from the high band-gap fluorene units in the core to low band-gap units in the linkage occurred, and light-emission could be controlled by adjusting the low band-gap chromophore. The ab initio modeling studies were carried out to investigate the steric effects of the core structure and side chains of the conjugated oligothiophene rings on their energy levels and band gaps, and to elucidate the PL properties observed in the present hyperbranched polymers. Preliminary results on double layer devices with configurations ITO/PEDOT/polymer (**4** or **7**)/LiF/Ca/Ag, which emitted blue and green light, respectively, are reported.

Results and Discussion

Synthesis and Characterization of Precursor 2 and Hyperbranched Polymers 3—9. During the past 20 years, hyperbranched polymers have drawn increasing interests in many areas including chemistry, materials science and biomedical research.[22] The obvious advantage of hyperbranched polymers over dendrimers lies in their synthetic simplicity, which generally involves one-step polymerization of AB_n-type ($n = 2-4$ in most cases) monomers.[23] Of particular recent interest has been the development of some Si-containing hyperbranched polymers as luminescent materials.[24] Compared with C-centered analogues, Si-centered materials exhibit superior performance with regard to quantum efficiency and film-forming ability.[21] A synthetic challenge for hyperbranched polymers is to prevent cross-linking of branches that would result in formation of insoluble networks during step-growth polymerization

Scheme 1. Synthesis of the Tetrabromoarylsilane Precursors 1 and 2

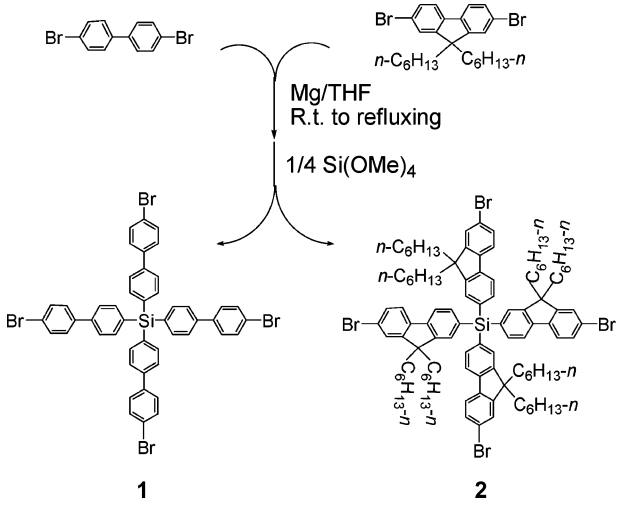

reaction. Such a tendency could be avoided or minimized when the polymerization is carried out below the gel point, that is, at a low concentration to prevent full conversion.[25]

The synthesis of the tetrabromo monomers **1** and **2** were achieved according to the method we reported recently (Scheme 1).[21] By using the fluorene units as the chromophoric arms, we anticipated that polymers derived from **2** would exhibit higher quantum efficiency than those from **1**. We could also investigate the steric effect of the tetrahedral core on the optical and thermal properties of the polymers. The syntheses involved preparation of the mono Grignard agents of 2,2′-dibromo-4,4′-biphenyl and 2,7-dibromo-9,9-dihexylfluorene, and subsequent substitution reactions between the Grignard agent and $Si(OMe)_4$. Preparations of **1** and **2** via the monolithiation of the two dibromides with *n*-BuLi tended to give butyl-substituted byproducts that involved a nucleophilic substitution between the monolithiate of the dibromides and *n*-BuBr.[20b] Compound **2** was obtained as a white solid in 45% yield. The ^1H NMR spectrum of **2** in $ClCD_2CD_2Cl$ showed two doublets [δ 7.49 (d, $^3J_{HH} = 8.0$ Hz, 4H); 7.59 (d, $^3J_{HH} = 8.0$ Hz, 4H)], one singlet [δ 7.50 (s, 4H)] and a broad peak at δ 7.74 (12 H) in the aromatic region, and the pattern of the NMR spectrum was not significantly changed upon heating the sample to 75 °C. The ^{13}C NMR spectrum of **2** in $CDCl_3$ exhibited 12 discrete aromatic-C peaks. The MALDI−TOF MS spectrum of **2** showed a strong molecular ion peak at 1667.3 (M^+). Compound **2** was well soluble in toluene, chloroform and THF but insoluble in ethanol and acetone. The DSC spectrum of **2** did not show melting/glass transition or crystallizing peaks upon heating it to 350 °C and cooling it to 50 °C. Wide-angle X-ray diffraction (WAXD) study revealed that **2** was amorphous in nature as only a broad amorphous peak was observed at ca. 20° in the WAXD spectrum. Compound **2** exhibited high thermal stability with a T_d of 415 °C and no weight loss at lower temperatures. The tetrabromo precursor emitted deep blue light with high PL quantum efficiencies in both solution and film state. This together with the amorphous nature, excellent thermal stability and synthetic simplicity would make **2** a good candidate as a novel molecular blue-emitter.[13,16]

The syntheses of polymers **3**−**9** are shown in Schemes 2−4. The polymers were synthesized by either Suzuki

Scheme 2. Synthesis of Polymers 3 and 4 by Suzuki Coupling Method

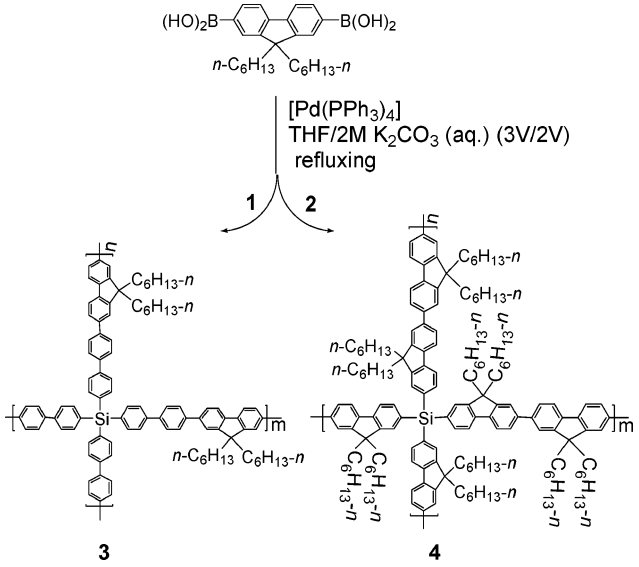

Scheme 3. Synthesis of Polymers 5 and 6 by Suzuki Coupling Method

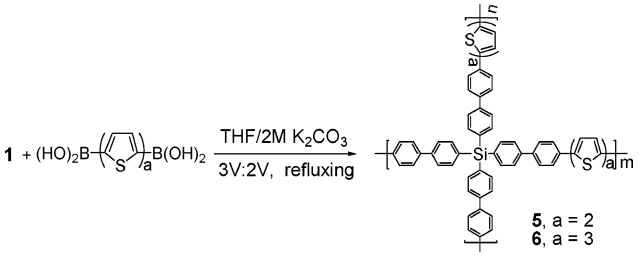

Scheme 4. Synthesis of Polymers 7−9 by the Grignard Coupling Method

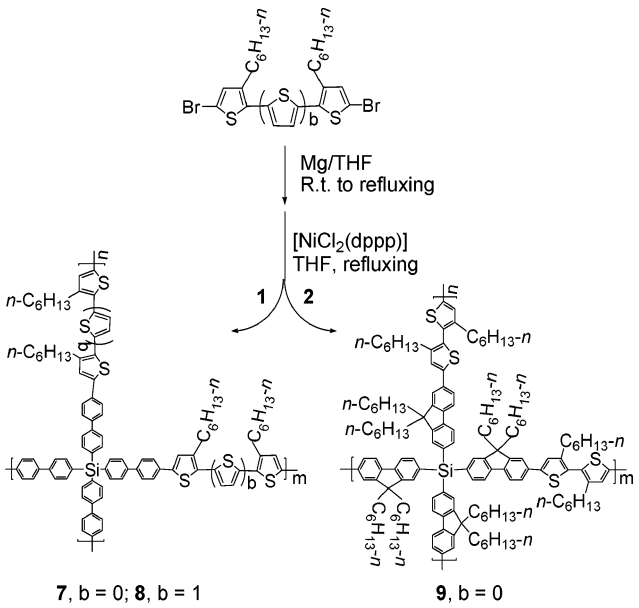

or Grignard coupling polycondensation reactions in dilute solutions to prevent cross-linking reaction, although such a reaction is relatively difficult to occur due to the rigid structures of the polymers.[21] The polymers were purified by two-step extractions: first with acetone to remove catalyst residues and unreacted monomers (soluble in acetone), and then with THF to extract the soluble polymers (cross-linked insoluble polymers were discarded). We found that only a small amount of cross-linked insoluble polymers were formed (15−20 wt % of soluble polymers). The obtained polymers were soluble in toluene and THF. In addition, polymers **7** and **8** exhibited good solubility in chloroform, whereas polymers derived from **2** were less soluble than their analogues of **1** despite presence of hexyl groups in the core. All polymers were satisfactorily characterized by ^{1}H and ^{13}C NMR spectroscopic studies (see Supporting Information). Elemental analyses of these polymers determined the residual % Br (from the bromo end groups) in the polymers to be 1.18−2.66%, which reveals the successes in the polymerization reactions. A summary of the synthesis, thermal, and optical properties of **2** and all polymers is given in Table 1. First, we synthesized two blue-light-emitting polymers **3** and **4** by Suzuki coupling method (Scheme 2). Under the same reaction condition, **3** was obtained as a gray powder in much higher M_w than **4**, which may be attributed to the less crowded structure of **1**. The ^{1}H NMR spectrum of **4** in $CDCl_3$ showed two CH_3 peaks at δ 0.75 and 0.85 at a ratio close to 1:2, which were from the core and linkage units, respectively, and is close to the monomer feed. Second, we synthesized polymers **5** and **6** that have varying conjugation lengths and emitted green and yellow lights in the solid state (Scheme 3). The ^{1}H NMR spectra of **5** and **6** in THF-d_8 showed a doulet of doublet (dd) signal at δ 7.07 (dd, J = 3.2 Hz, J' = 5.2 Hz) and 7.11 (dd, J = 3.2 Hz, J' = 4.4 Hz), which were assigned to the β-H of bithiophene and terthiophene moieties at the terminal groups, respectively. The M_w values of polymers **5** and **6** were significantly lower than those of **3** and **4**, probably due to their less solubility in THF. To improve the solubility of the fluorene-oligothiophene hyperbranched polymers, we synthesized polymers **7** and **8** with hexyl groups on the thiophene rings (Scheme 4). We first tried to synthesize the diboronic acids from the dihexylbithiophene and -terthiophene and their dibromo derivatives by standard lithiation−boration method[26] but failed, probably due to the presence of hexyl groups that makes the α-H less acidic. In consideration that electron-donating hexyl groups can enhance the reactivity of dibromides of thiophenes to form Grignard agent, we used the Grignard coupling method to synthesize **7** and **8** by a longer reaction time. We synthesized polymer **9** by the same method to further investigate the core effect on the optical and thermal properties of the polymers. M_w determinations showed that the Grignard coupling polycondensation reactions were successful. The ^{1}H NMR spectra of **7** and **8** showed different patterns from those of **5** and **6**. For example, the ^{1}H NMR spectrum of **7** in $CDCl_3$ showed a doublet signal at δ 6.99 (J = 5.2 Hz) that was from the β-H of the dihexylbithiophene at the terminal groups, instead of dd signals of similar protons in polymers **5** and **6**. Similar to **4**, polymer **9** was less soluble in chloroform than **7** and **8**. The ^{1}H NMR spectrum of **9** in $ClCD_2CD_2Cl$ exhibited two CH_3 peaks at δ 0.84 and 1.03, and two Ar−CH_2 peaks (C−CH_2 from fluorene and thienyl-CH_2 of bithiophene) at δ 1.96 and 2.50 with a ratio close to the monomer feed (2:1). Polymers **3**−**9** exhibited good thermal stability with their T_gs being over 176 °C and T_ds over 305 °C, and no weight losses were observed at lower temperatures. In addition, polymers **4** and **9** (derived from **2**) exhibited higher T_ds than their analogue polymers **3** and **7** (derived from **1**). The hyperbranched polymers exhibited significantly higher T_gs than their linear analogues.[2] It is noteworthy that high

Table 1. Summary of the Synthesis, Thermal, and Optical Properties of 2−9

	yield (%)	M_w[a] (PD)	T_g[b] (°C)	T_d[c] (°C)	solution			film		
					absorption[d] (log ϵ)	emission[e] (fwhm)	ϕ_{PL}[f]	absorption	emission[e] (fwhm)	ϕ_{PL}[f]
2	45		*h*	415	319 (5.35), 335 (4.09)[g]	398, 377 (60)	1.20,[i] 0.33	319, 334[g]	403 (51)	0.48,[i] 0.17
3	58	10 680 (2.08)	236	376	350	406, 426 (46)	0.99	357	419, 437 (51)	0.84
4	55	6280 (1.11)	196	385	315, 335[g]	403 (51)	1.44,[i] 0.40	316, 344[g]	411, 426 (52)	1.05,[i] 0.67
5	52	4570 (1.24)	226	311	360	435 (68)	0.27	361	510 (126)	0.04
6	49	4680 (1.51)	228	316	397	485, 456 (88)	0.25	401	582, 539 (143)	0.05
7	36	8080 (1.88)	236	356	359	468 (84)	0.21	372	496 (90)	0.22
8	31	8700 (2.01)	233	305	401	531, 512 (108)	0.20	421	638 (120)	0.03
9	33	6360 (1.23)	176	411	316, 338[g]	394, 374 (48)	0.84,[i] 0.23	317, 340[g]	490, 397 (165)	0.08,[i] 0.02

[a] Measured by GPC in THF using polystyrene as standards. [b] The middle temperature. [c] T_d is defined as the temperature at which a 5% weight loss is recorded by the TGA analysis. [d] Concentration for **2** is in 1×10^{-7} M and for polymers were 0.2 mg in 10 mL THF. [e] The excitation wavelengths were their respective strongest long wavelength absorption maximum. [f] The photoluminescence quantum yields (Φ_{PL}) of the compounds in THF were determined using a solution of quinine sulfate (ca. 1×10^{-5} M in 0.1 M H_2SO_4, having a quantum yield of 0.55) as a standard. The Φ_{PL} values of films were determined using 9,10-diphenylanthracene (dispersed in PMMA films with a concentration lower than 1×10^{-3} M and a quantum efficiency of 0.83) as a standard. [g] Shoulder peaks. [h] Not observed. [i] Excited at long wavelength shoulder peaks. fwhm: full width at half-maximum.

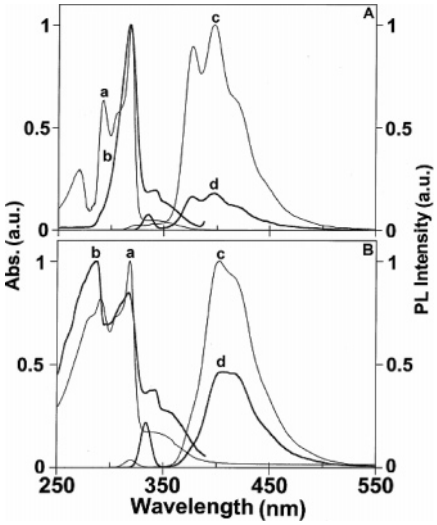

Figure 1. UV and PL spectra of compound **2** in THF solution (A) and the solid state (B). Key: (a) UV spectra; (b) excitation spectra; (c and d) emission spectra excited at 318 and 334 nm, respectively (spectra d are normalized relative to those of c).

glass transition temperatures and high decomposition temperatures are important for an organic luminescent material to be used for practical applications in OLEDs.[27]

Optical Properties of 2—9 in Solution and the Solid State. The UV and PL properties of **2**−**9** in THF solution and the film state were investigated. Uniform transparent thin films were prepared on quartz substrates by spin-coating from toluene solutions (about *wt.*1%) at a spin rate of 2000 rpm. The absorption, PL emission and excitation spectra of **2** are shown in Figure 1. The solution and film absorption spectra of **2** exhibit a same maximum at 319 nm with long wavelength tailing to 400 nm. The peak at 319 nm is red shifted from that of 2-bromo-9,9-dihexylfluorene (309 nm) in the same solvent, and belong to the $\pi \rightarrow \pi^*$ excitation of the fluorene arms. The long wavelength tailing may be attributed to a delocalized chromophore involving a hyperconjugation via the central δ-Si atom.[28] The solution and film PL excitation spectra of **2** exhibit an obvious long wavelength peak at 335 nm. Excitation of the solution and film sample at 319 and 335 nm, respectively, give PL emission spectra with the same pattern and emission maxima but different intensities. The emission maximum of **2** in film state is slightly red shifted from that of solution (403 vs 398 nm), but its fwhm value becomes even smaller (51 vs 60 nm).

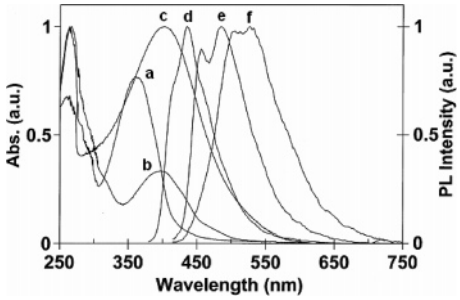

Figure 2. UV (a−c) and PL emission spectra (d−f) of poylmers **5**, **6**, and **8** in THF solution, respectively.

Furthermore, no excimer-like green-light-emitting peak is observed in the PL spectra. This together with the good film quantum efficiency indicates that concentration quenching is not serious in the solid state of the molecular glass-forming compound.

Figure 2 shows the UV and PL spectra of polymers **5**, **6**, and **8** in THF solutions. Both the absorption and emission maxima of polymers **6** and **8**, which have longer conjugation lengths, are significantly red shifted from those of **5**. The absorption maxima of **6** and **8** are similar, but the emission maximum of **8** is red shifted from that of **6** and can be attributed to the electron-donating hexyl groups. The polymers emitted deep blue to green light in solution with the PL quantum efficiencies being in the range 0.20−0.27 and fwhm values of 68−108 nm. The film emission maxima of these polymers were markedly red shifted (75−107 nm) from those of their solution ones. The film PL spectra also showed increases in fwhm values (12−58 nm). The films of **5**, **6**, and **8** emitted visible green, yellow and red light, respectively, with dramatic decreases in quantum efficiencies. These results show that concentration quenching happened in the films of these polymers, which is in contrast to fluorene-containing analogues,[21] and may be attributed to less efficient oligothiophene fluorophores and their more flexible structures. For the polyfluorene **3**, its three-dimensional structure and bulky hexyl groups at the C-9 position both make the intermolecular interactions more difficult, and thus reduce concentration quenching of fluorescence.[7−12]

A comparison of the optical properties of polymers **3**/**4** and polymers **7**/**9**, which have the same linkage units but different cores, respectively, reveals that the tetrahedral core plays an important role on the optical properties of the hyperbranched polymers. The solution and film absorption and PL spectra of polymers **3** and

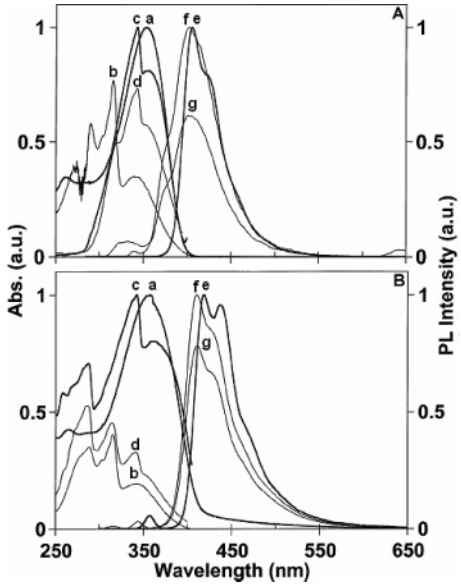

Figure 3. UV and PL spectra of poylmers **3** and **4** in THF solution (A) and the solid state (B). UV spectra of polymer **3** (a) and polymer **4** (b). Excitation spectra of polymer **3** (c) and polymer **4** (d). Emission spectra of polymer **3** (e) and polymer **4** (f and g). The spectra f and g were excited at 334 and 316 nm, respectively, and the spectra g were normalized relative to those of f.

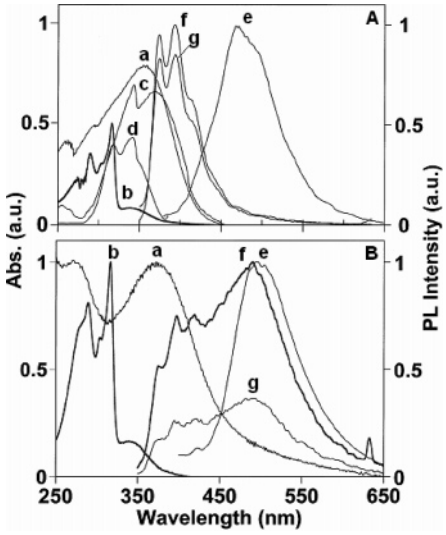

Figure 4. UV and PL spectra of poylmers **7** and **9** in THF solution (A) and the solid state (B). The UV spectra of polymer **7** (a) and polymer **9** (b). Excitation spectra of polymer **7** (c) and polymer **9** (d). Emission spectra of polymer **7** (e) and polymer **9** (f and g). Spectra f and g were excited at 340 and 317 nm, respectively, and spectra g were normalized relative to spectra f.

4, which were derived from **1** and **2** with 9,9-dihexylfluorene, respectively, are shown in Figure 3. The UV spectra of **3** show an unstructured absorption maximum at 350 (solution) and 357 nm (film), which are dramatically red shifted from 9,9-disubstituted fluorene (typically around 318 nm), indicating the presence of electron delocalization within fluorene and biphenyl. The UV spectra of **4** show two long wavelength peaks at 315 and 335 nm (solution) and 316 and 344 nm (film) with the former being stronger. The former peak is assigned to the $\pi \rightarrow \pi^*$ excitation of the fluorene units, whereas the latter involves the electron delocalization in the chromophoric arm.[28] Excitation of the solution and film samples of **4** at the two long wavelength absorption peaks give similar emission spectra peaking at 403 (solution) and 411 nm (film) with different intensities. It is important to note that both the absorption and emission maxima of **4** in solution and the solid state are slightly blue shifted from those of **3**, indicating a less efficient electron delocalization among the fluorene units in **4** than the fluorene and biphenyl units in **3**. Such a weaker electron delocalization in **4** should be attributed to the more crowded structure of the tetrahedral core, which results in larger torsion angles among the fluorene rings. Polymers **3** and **4** emitted deep blue light highly efficiently in both solution and the solid state. The other noteworthy features include the following: (1) small red shifts (8−13 nm) of the emission maxima in the film PL spectra relative to the solution PL spectra; (2) small fwhm values (46−52 nm) for both solution and film emission spectra; (3) absences of long wavelength green-light-emission peaks; (4) higher quantum efficiency of **4** than **3**. These optical data together with their excellent thermal stability (high T_g and T_d) indicate that polymers **3** and **4** are excellent blue-light-emitting materials.

The solution and film absorption and PL spectra of polymers **7** and **9** are shown in Figure 4. The UV spectra of **7** show structureless peaks at 359 (solution) and 372 nm (film), which are significantly red shifted from dihexylbithiophene (292 nm, THF), indicating that effective electron delocalization is present within the two units. Similar to the UV spectra of **4**, the UV spectra of **9** exhibit two long wavelength peaks at 316 and 338 (solution) and 317 and 340 nm (film) with the former being stronger. The PL excitation spectrum of **9** exhibits two long wavelength peaks at 318 and 342 nm with the latter being stronger. The two peaks could be assigned to the fluorene chromophore and the electron-delocalized chromophoric arm, respectively. Polymer **7** emitted blue and green light with emission maxima peaking at 468 and 496 nm in THF and the condensed state, respectively. The emission of **7** in the solid state was not quenched as similar solution and film quantum efficiencies being recorded (0.21 vs 0.22). Excitation of the solution sample of **9** at 317 and 340 nm, respectively, gave similar structured emission spectra peaking at 394 nm. This emission is typical for the fluorene chromophore and the emission from the electron-delocalized chromophore is suppressed. Excitation of the film sample of **9** at 317 and 340 nm, however, emitted visible green light, and its PL spectra clearly show both emissions from the fluorene and dihexylbithiophene chromophores. The film PL emission spectra of **9** show a strongly unstructured peak at 490 nm and a weaker structured peak at 397 nm. These results show that electron delocalization of **9** at the excited state is not effective and the fluorene and dihexylbithiophene behave independently. The different solution and film PL properties of **9** are perhaps due to different band gaps of dihexylbithiophene chromophore in solution and the condensed state. Ab initio studies showed that dihexylbithiophene has slightly higher band gap than dihexylfluorene in dilute solution (see the section Ab Initio Studies), and this explains why the PL spectra of **9** only showed the emission peaks from fluorene units. In the condensed state, however, a more coplanar positioning of the two thiophene rings due to the packing effects increased their electron delocalization and lowered the band-gap of dihexylbithiophene.[30] As a result, the band gap of dihexylbithiophene becomes lower than that of dihexylfluorene, which results in green-light emission

Chart 2. Structures of Model Compounds for ab Initio Studies

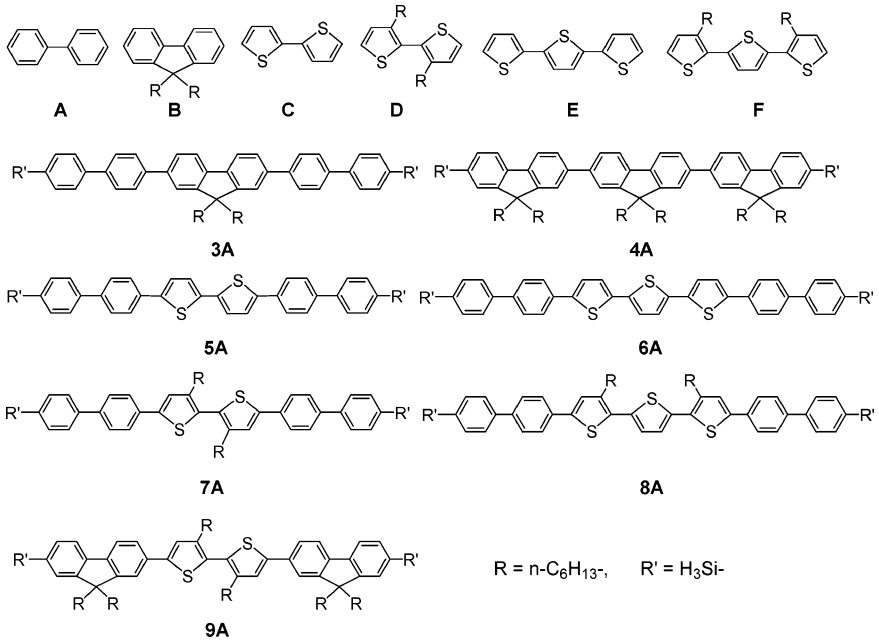

Table 2. Calculated and Determined Band Gaps of the Model Compounds

compd	band gap (eV)	torsion angles (deg)[c]	compd	band gap (eV)	torsion angles (deg)[c]
A	3.934	41.5	**3A**	2.636 (3.10[b])	−40.1, −36.7, −0.2, 38.2, −37.5
B	3.568	0.5	**4A**	2.516 (3.12[b])	−0.1, −36.0, −0.0, 37.9, −0.7
C	2.897	19.8	**5A**	2.029 (2.76[b])	−39.2, 23.0, −18.5, −22.6, 38.1
D	3.725	72.0	**6A**	1.797 (2.42[b])	39.6, 23.2, 18.5, −13.9, −22.4, −39.0
E	2.279	21.0, −18.4	**7A**	2.345 (2.82[b])	37.4, −22.9, 59.6, −23.9, −38.2
F	2.518	45.0, −28.0	**8A**	1.863 (2.15[b])	40.0, −14.4, −20.0, 35.2, −23.2, 37.8
1	3.488 (3.60[a])	−42.1, 42.1, 38.9, −40.2	**9A**	2.222 (3.04[b])	−0.1, −22.7, 52.4, −26.5, −0.6
2	3.113 (3.22[a])	−1.4, 1.5, −0.2, 0.3			

[a] Estimated from the onset wavelengths of UV spectra in dilute THF solution ($A < 0.2$). [b] The band gaps of the corresponding hyperbranched polymers estimated from their onset wavelengths of their solution UV spectra. [c] Optimized torsion angles of Ar−Ar′ rotations from left to right (see Chart 2).

from the low band-gap dihexylbithiophene and energy transfer from fluorene units to dihexylbithiophene units. In consideration that molar ratio of fluorene/bithiophene is 2:1 and fluorene is a more efficient fluorophore than oligothiophenes while PL intensity of green is higher, we conclude that intramolecular energy transfer from the fluorene units to the bithiophene units occurred.[4]

Ab Initio Modeling Studies. Ab initio/DFT studies provide further information regarding the steric effects of the core and linkage structures on the optical property of the present hyperbranced polymers. It has long been established that introduction of long aliphatic chains into conducting polymer (CP) backbones can increase their solubility in organic solvents as well as improve their solution processability.[31] Few studies have been carried out to investigate the effect of side chains on the energy levels of CPs.[32] Our present studies clearly show that the core and linkage structures have profound effects on the optical properties of the present hyperbranched polymers. We thus investigated the steric effects of side chains on the optical properties of CPs (particularly oligothiophenes) by ab initio studies. Chart 2 shows the structures of model compounds **3A**−**9A**, which have chromophoric units similar to those of their respective hyperbranched polymers. The calculated band gaps and optimized torsion angles of all the model compounds are summarized in Table 2.

The HOMO and LUMO orbitals and optimized conformations of the two tetrahedral precursors are shown in Figure 5. The calculated band gaps of **1** and **2** are quite close to the values obtained from the onset wavelengths of solution UV spectra. The HOMO orbitals of **1** and **2** are localized on the rings and Br atoms, whereas their LUMO orbitals are delocalized. Moreover, the LUMO of **1** is more symmetric in the 3-D space than that of **2**, which is mainly localized on one arm. Such an asymmetric electron distribution of **2** at its excited state is perhaps due to the larger band-gap difference between fluorene and δ-Si and its more crowded structure, which makes the interarm electron delocalization more difficult than for **1** and may also account for the observed core effect on the optical properties of present polymers.

Second, we investigated the effect of side chains of oligothiophenes on the energy levels and band gaps of homo- and hetero-oligothiophenes. We found that the hexyl groups at thiophene rings increase band gaps. For example, **D** shows a significantly higher band gap and torsion angle than **C**, which resulted from the repulsion between the neighboring hexyl groups. A further disposition of the two hexyl groups in **F** results in less significant increases in band gap and torsion angle relative to **E**. The ab initio studies of model compounds **3A**−**9A** reveal that (1) the hexyl groups at the thiophene rings tend to increase torsion angles and the band gaps of these hetero-chromophoric compounds and (2) effective electron-delocalization only occurs on four consecutive conjugated rings and centers on the middle rings.

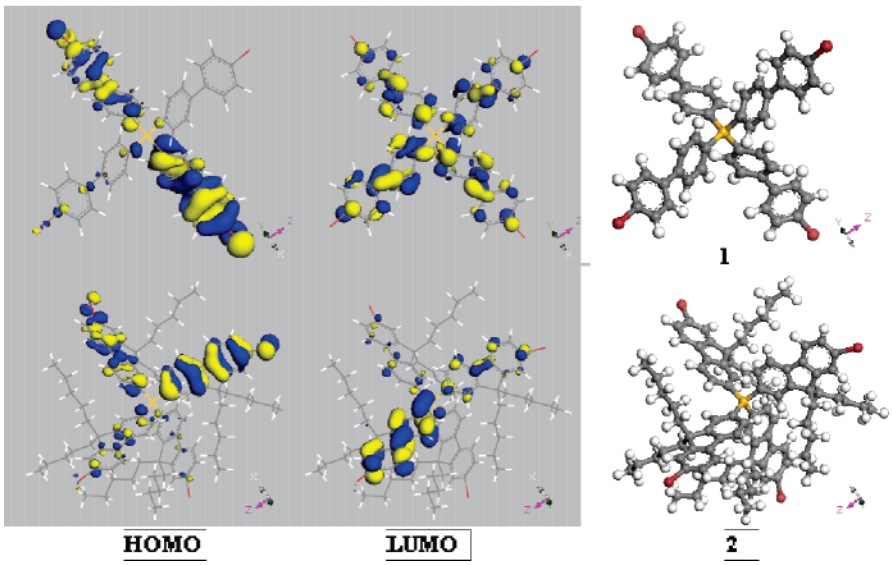

Figure 5. HOMO/LUMO orbitals and optimized conformations of tetrahedral compounds **1** and **2**.

Table 3. Effect of Torsion Angle on the Energy Level of Model Compound 4A′

torsion angle (deg)	total energy (ha)	HOMO	LUMO	gap (eV)	λ (nm)	torsion angle (deg)	relative energy (kcal/mol)
90	−2318.9708565	−5.259	−1.949	3.310	374.6	90, 90	3.859882
80	−2318.9711506	−5.193	−1.993	3.200	387.5	80, 80	3.675343
70	−2318.9726480	−5.096	−2.085	3.011	411.8	70, 70	2.735769
60	−2318.9746634	−5.015	−2.173	2.842	436.3	60, 60	1.471166
50	−2318.9763628	−4.945	−2.253	2.692	460.6	50, 50	0.404844
40	−2318.9769067	−4.887	−2.331	2.556	485.1	40, 40	0.063563
optimized	**−2318.9770080**	**−4.875**	**−2.348**	**2.527**	**490.7**	**37, 37.7**	**0**
30	−2318.9761307	−4.844	−2.394	2.450	506.1	30, 30	0.550479
20	−2318.9746081	−4.810	−2.452	2.358	525.9	20, 20	1.505865
10	−2318.9724968	−4.787	−2.495	2.292	541.0	10, 10	2.830643

For example, compounds **7A** and **8A** (containing hexyl groups at thiophene rings) exhibit 0.06 and 0.32 eV higher band gaps than their analogue compounds **5A** and **6A**, respectively, and the effect of hexyl groups of **8A** is much weaker than those of **7A** due to a longer distance between the two groups. Figure 6 shows the HOMO/LUMO orbitals and optimized conformations of model compounds **3A**−**9A**. The HOMOs are localized on rings in the middle section while the LUMOs are delocalized to several aromatic rings. The effective electron delocalization occurs in three to four consecutive aromatic rings no matter how long the conjugation length is. A comparison of the calculated band gaps of model compounds **3A**−**9A** with the UV-derived band gaps of hyperbranched polymers **3**−**9** show that all the hyperbranched polymers have dramatically higher band gaps than their respective model chromophoric compounds (0.29−0.88 eV). These results indicate that the rigid structures and side chains greatly decrease the efficiency of electron delocalization in the chromophoric arm in these polymers and thus increase their band gaps. Such a reduced electron delocalization effect should be attributed to the increase in torsion angles of aromatic rings. For example, the torsion angle between the two thiophene rings in **7A** is 59.6°, which is dramatically higher than that in **5A** (18.5°) and accounts for the higher band gap of **7A**.

To correlate the energy levels of the present model compounds with torsion angles, we calculated the energy levels of compound **4A′** (Table 3 and Figure 7). We found that the optimized torsion angles of **4A′** (37, 37.7) are similar to those of compound **4A** (36, 37.8), indicating the effect of substituents at C-9 of fluorene is much weaker than those directly attached to aromatic carbon atoms. It can be seen that, with the increase in torsion angles, the HOMO level decreases whereas the LUMO level increases, both almost linearly, resulting in the increase in the band gap. From the UV-derived band gap of polymer **4** (3.12 eV), we estimate that the torsion angles of the conjugated arms in **4** are around 80°. Such large torsion angles are apparently resulted from the rigid and hyperbranched structure of **4** and would prevent effective electron-delocalization from occurring. Such a highly unparallel disposition of the three conjugated fluorene rings in **4** would render them to behave independently at excited state and explains the even blue shift of emission maxima of **4** relative to that of **3**. Similar calculations on the energy levels and band gaps of **D** show the same trend as **4A′** (see Supporting Information). For example, the band gap of **D** at a torsion angle of 15° is 2.895 eV, which is 0.83 eV lower than the optimized value (72°). Since the fluorene unit has a fixed conformation and is located at the core, it is reasonable to assume that its band gap in film state is similar to that in solution. In contrast, a decrease in the torsion angle (i.e., from 72 to 15°) of the thiophene rings of **D** moiety in **9** would dramatically lower its band gap to allow the differentiation of band gaps of the two chromophores and the intramolecular energy transfer to occur. This finding is important, as we can realize long wavelength light emission by incorporating low band-gap chromophore into the hyperbranched polymers and tuning light emission by intramolecular energy transfer.

Electroluminescence Properties. In view of good optical and thermal performance of the blue-light-

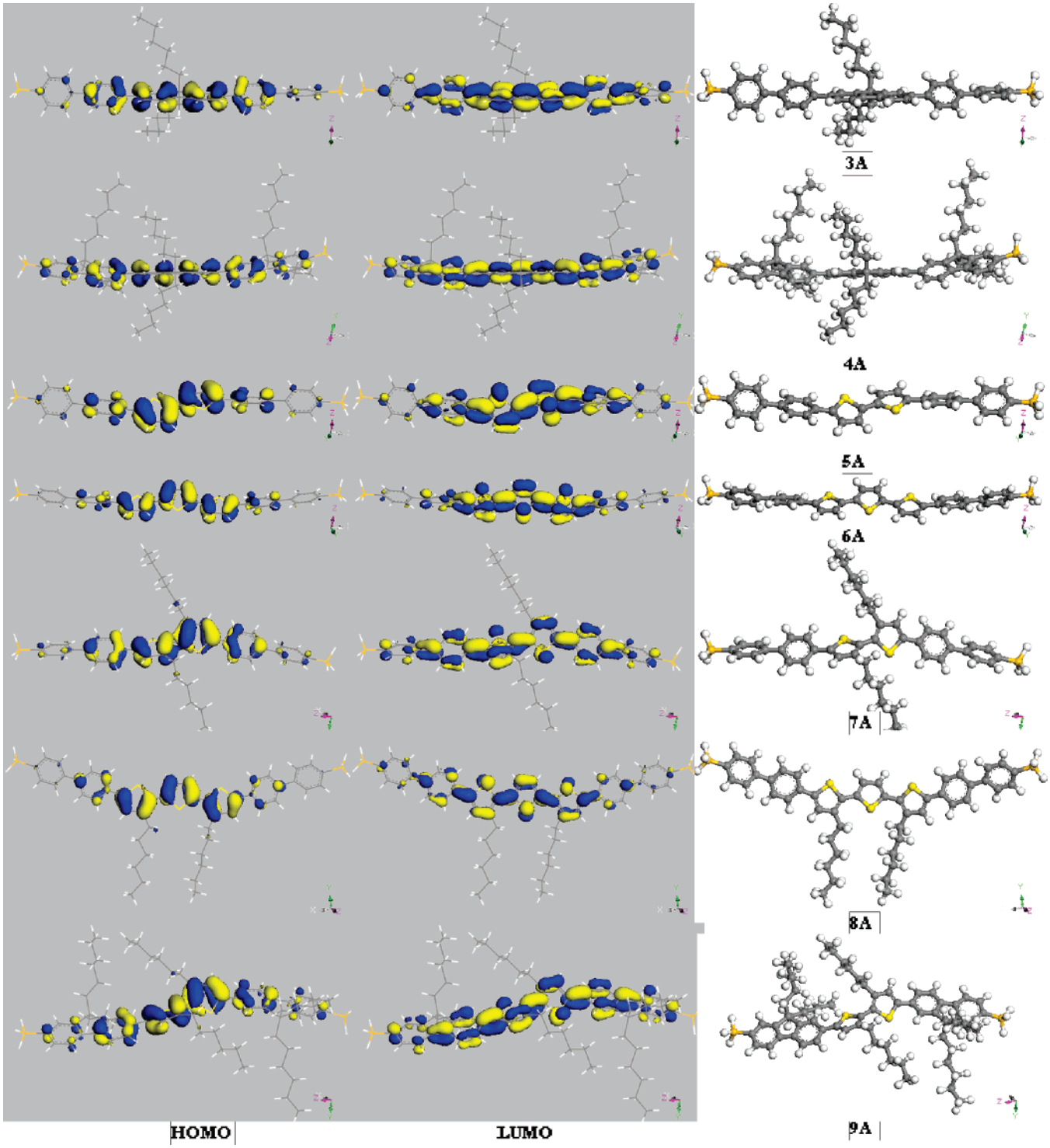

Figure 6. HOMO/LUMO orbitals and optimized conformations of model compounds **3A**−**9A**.

emitting polymer **4** and green-light-emitting polymer **7** in the solid state, we carried out preliminary studies on their application for polymeric electroluminescent diodes. Polymers **4** and **7** were used as the emitting layers in double-layer light-emitting devices with configurations ITO(130 nm)/PEDOT(82 nm)/polymer **4** or **7** (80 and 100 nm, respectively)/LiF(0.5 nm)/Ca(20 nm)/Ag(100 nm). Poly(3,4-ethylenedioxythiophene) (PEDOT) doped with poly(styrenesulfonic acid) (PPS) was used as the hole injection/transporting layer. The active area of the device was about 4.0 mm^2. Figure 8 shows the current−voltage and luminance−voltage characteristics of the devices. The device performance data are listed in Table 4. The device of **4** emitted bright blue light starting at about 9.6 V and reaches a brightness of 167 cd/m^2 at a bias of 15.2 V. The obtained maximum current efficiency was 0.78 Cd/A (at 15.2 V with current density of 21.5 mA/cm^2 and a brightness of 167 cd/m^2). The EL spectrum of the device exhibited emission peaks at 426 and 446 with similar intensities and a fwhm of 68 nm, which are very similar to its film PL spectrum, indicating that same excitations are involved in both cases (Figure 9).[33] In addition, a weak peak at 500−550 nm, which is typical of PFs due to excimer formation,[2,3] is also observed. Furthermore, the EL spectra of the device obtained by operating at up to 20 V were

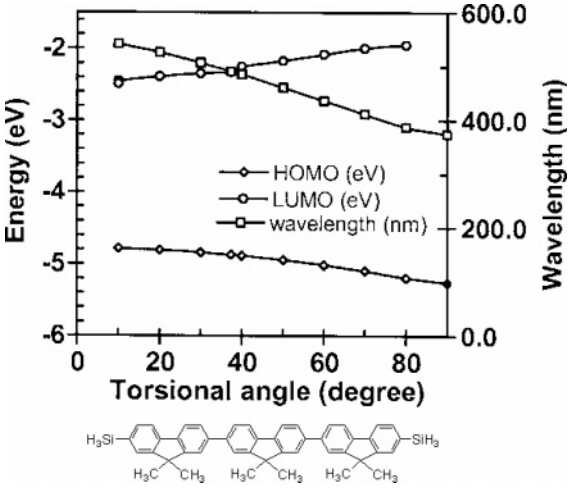

Figure 7. Effect of torsion angle on the energy level of model compound **4A′**.

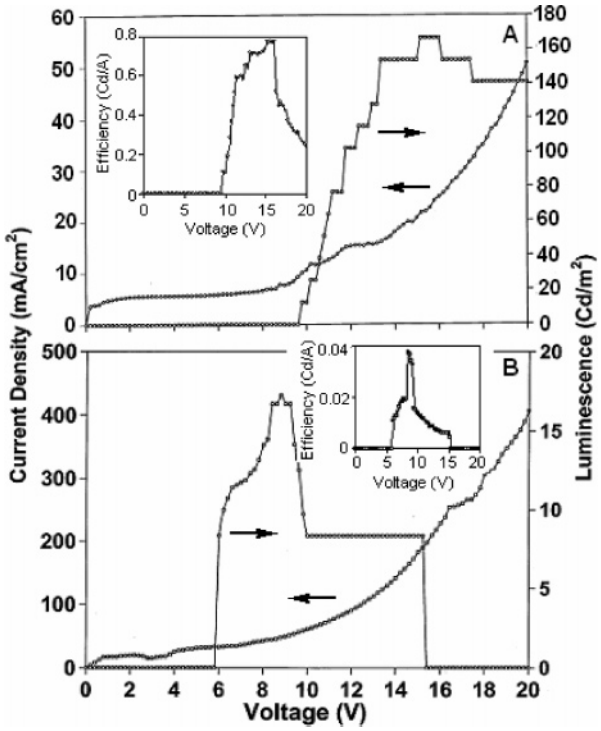

Figure 8. Current−voltage and luminance−voltage characteristics of the blue- and green-light-emitting devices prepared from polymers **4** (A) and **7** (B), respectively. Insets: the current efficiency curves of the devices.

Table 4. Performances of ITO/PEDOT/Polymer/LiF/Ca/Ag Electroluminescent Devices (Data in Parentheses are Operating Voltage/V)

polymer	turn-on voltage, V	maximum luminescence, Cd/m^2	maximum current density, /mA/cm^2	maximum current efficiency, Cd/A
4	9.6	166.75 (15.2)	21.54 (15.2)	0.78 (15.2)
7	5.8	17.23 (8.8)	47.14 (8.8)	0.04 (8.8)

similar in spectral patterns with slightly decreasing intensities. The device of **7** emitted visible green light starting at about 5.8 V and reaches a brightness of 17 cd/m^2 at a bias of 8.8 V. The maximum current efficiency was measured to be 0.04 Cd/A (at 8.8 V with current density of 47 mA/cm^2 and a brightness of 17 cd/m^2). The EL spectrum of the device obtained at 9.0 V showed an emission maximum around 530 nm. These preliminary data show the applicability of the present novel polymers as PLED blue- and green-emitters. Detailed studies on device fabrication and performance are currently in progress.

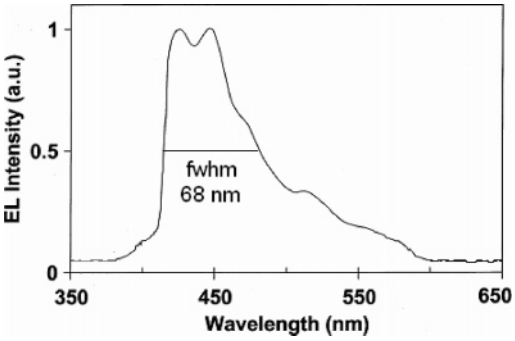

Figure 9. EL spectrum of the blue-light-emitting device with the configuration glass/ITO/PEDOT/ polymer **4**/LiF/ Ca/Ag operated at 12 V.

Conclusion

We report in this paper the synthesis of hyperbranched alternating copolymers from two AB_4-type tetrabromo monomers (**1** and **2**) of different band gaps and steric hindrances with AB_2-type monomers of 9,9-dihexylfluorene and oligothiophenes via either Grignard or Suzuki coupling polycondensation reactions. These polymers exhibited high thermal stabilities with T_gs being over 170 °C and T_ds over 300 °C. The core structures exhibit intrigue effects on the optical properties of the hyperbranched polymers. The electron-delocalization in the chromophoric arm of polymers derived from **1** was observed and light emission could be tuned by controlling the conjugation length. In contrast, the torsion angles between aromatic rings in the chromophoric arm of polymers derived from **2** are high and electron-delocalization in the chromophoric arm was not effective. As such, light emission could be tuned by intramolecular energy transfer from high band-gap fluorene units in the core to low band-gap units in the linkage. The effects of side chains of homo- and hetero-oligothiophenes, and of steric hindrance of tetrahedral core on the energy levels and band gaps of some model oligomers and the present hyperbranched polymers were investigated by ab initio studies. RGB emissions in the film state were achieved from the present hyperbranched polymers and preliminary studies on the fabrication and performance of a blue-light-emitting and a green-light-emitting device are reported. We are currently synthesizing more efficient green to red emitting hyperbranched polymers from tetrahedral core **2** and realize the emissions by the intramolecular energy transfer presenting in such unique structures.

Experimental Section

General Information. Unless stated otherwise, all reagents and solvents were of commercial grade and used as received. All reactions were performed under a purified nitrogen atmosphere using the standard Schlenk technique. Tetrahydrofuran (THF) was distilled over CaH_2 before use. The ^{1}H and ^{13}C NMR spectra were recorded at 25 °C on a Bruker AVANCE 400 spectrometer at 400 and 100 MHz, respectively. The mass spectrum of **2** was recorded on an ABI Voyager STR MALDI−TOF MS spectrometer. UV−vis spectra were measured with a UV−vis spectrometer (Shimadzu, UV-2501 PC)

at 20 °C. Fluorescence spectra were recorded on a LS50B Luminescence spectrometer (Perkin-Elmer) at 20 °C. Glass transition temperatures were determined by differential scanning calorimetry (DSC) experiments using a TA 2920 modulated DSC instrument with a ramp speed of 10 °C/min. Thermogravimetric analyses (TGA) were conducted on a Perkin-Elmer thermogravimetric analyzer TGA 7 under a heating rate of 20 °C/min and a nitrogen flow rate of 20 cm^3/min. The photoluminescent quantum yields (Φ_{PL}) of the compounds in THF were determined using a solution of quinine sulfate as a standard (ca. 1×10^{-5} M in 0.1 M H_2SO_4, having a quantum yield of 0.55). The Φ_{PL} values of films were determined using 9,10-diphenylanthracene as a standard (dispersed in PMMA films with a concentration lower than 1×10^{-3} M and a quantum efficiency of 0.83). WAXS measurements were conducted using Bruker X-ray diffractometer using Cu Kα (λ = 1.541 Å) radiation. Thin films of the samples prepared by a hydraulic press die were used for the measurements. The X-ray tube was operated at 40 kV and 40 mA. Elemental analyses were performed by the Elemental Analysis Laboratory of the Department of Chemistry at the National University of Singapore.

The starting compounds 2,7-dibromo-9,9-dihexylfluorene,[34a] 9,9-dihexylfluorene-2,7-diboronic acid,[34b] 2,2′-bithiophene-5,5′-diboronic acid,[35a] 2,2′:5′,2″-terthiophene-5,5″-diboronic acid,[35a] 5,5′-dibromo-3,3′-dihexyl-2,2′-bithiophene,[35b] 5,5″-dibromo-3,3′-dihexyl-2,2′:5′,2″-terthiophene,[35b] and tetra(4-bromobiphenyl)-silane[21] were prepared according to literature methods.

Synthesis of Tetra(2-bromo-9,9-dihexylfluorene-7-yl)-silane (2). 2,7-dibromo-9,9-dihexylfluorene (12.5 g, 25.4 mmol) and magnesium turnings (0.62 g, 25.4 mmol) were dissolved in dry THF (150 mL). The Grignard reaction was initiated by addition of I_2. The reaction mixture was first stirred at room temperature for 2 h, and then was heated at 65 °C overnight to give a brown solution of the Grignard reagent. To a solution of $Si(OMe)_4$ (1.33 g, 6.4 mmol) in 50 mL THF was added the Grignard agent at room temperature. The reaction mixture was stirred at room temperature for 16 h, and then refluxed for 4 h. Upon completion, 100 mL of 1 N HCl was added slowly into the reaction mixture. The organic layer was isolated and the aqueous layer was extracted with dichloromethane (2 × 150 mL). The combined organic solution was washed with brine and dried ($MgSO_4$). Filtration through Celite gives a clear yellow solution. Removal of the solvent afforded the crude product as a yellow solid. The product was first washed with acetone using a Soxhlet apparatus for 24 h to remove unreacted starting materials, and then purified by silica gel column chromatography (*n*-hexane/chloroform 2:1, R_f = 0.45). The product was obtained as a white solid in 45% yield (4.8 g). Anal. Calcd for $C_{100}H_{128}Br_4Si$: C, 71.59; H, 7.69; Br, 19.01. Found: C, 71.28; H, 7.52; Br, 19.45. ^{1}H NMR ($ClCD_2CD_2Cl$): δ 0.73 (br, 24 H); 1.06 (br, 48 H); 1.19 (br, 16 H), 1.96 (m, 16 H); 7.49 (d, $^3J_{HH}$ = 8.0 Hz, 4H); 7.50 (s, 4H); 7.59 (d, $^3J_{HH}$ = 8.0 Hz, 4H); 7.70−7.88 (br, 12H). The spectral pattern did not show significant change upon heating the sample to 75 °C. ^{13}C NMR ($CDCl_3$): δ 14.4, 23.0, 26.0, 29.7, 30.2, 40.6, 55.4, 120.3, 121.5, 121.8, 126.5, 130.1, 130.5, 133.6, 134.7, 139.4, 143.1, 150.6, 152.9. MS (MALDI−TOF), *m/e*: 1667.3 (M^+).

A General Procedure for the Suzuki Coupling Reactions, Synthesis of Polymers 3—6. Tetrabromoarylsilanes **1** or **2** (1.0 g), the diboronic acid of 9,9-dihexylfluorene or oligothiophenes (Schemes 2 and 3) (2.0 equiv), [$Pd(PPh_3)_4$] (1 mol %) were dissolved in THF (150 mL) and 2 M K_2CO_3 (aqueous, 110 mL). The reaction mixture was degassed by bubbling with N_2, and then was refluxed for 16 h under N_2. Upon completion, the THF layer was separated. After removal of THF, the solid was washed with water and ethanol. The dried product was washed with acetone using a Soxhlet apparatus for 72 h to remove the catalyst residues and oligomers. The solid residue was then extracted with THF using a Soxhlet apparatus for 24 h, and the insoluble solid (cross-linked networks) was discarded. Removal of THF gave the soluble hyperbranched polymer product. The products were dried in a vacuum oven at 120 °C for 3 days.

Polymer 3. A light-yellow powder 0.75 g (55%). The NMR and microanalysis data were the same as the results we reported previously.[21]

Polymer 4. A light-yellow solid 0.88 g (72%). Anal. Calcd for $(C_{150}H_{192}Si)_n$: C, 89.04; H, 9.57. Found: C, 87.98; H, 10.25; Br, 1.18. ^{1}H NMR ($CDCl_3$): δ 0.75 (m, 12 H), 0.85 (m, 24 H), 1.07 (m, 32 H), 1.22 (m, 64 H), 1.95 (m, 24 H), 6.56 (s), 6.98 (s), 7.21 (s); 7.28−7.35 (m, 8H), 7.40−7.90 (m, 28 H). ^{13}C NMR (THF-d_8): δ 14.9, 15.1, 24.0, 24.2, 30.9, 31.3, 33.1, 33.5, 41.8, 56.5, 111.2, 115.0, 115.3, 120.3, 121.0, 121.2, 122.5, 124.1, 127.5, 128.0, 128.1, 128.2, 128.4, 129.7, 130.6, 134.4, 135.0, 135.9, 142.0, 142.5, 144.2, 151.5, 152.3, 153.1.

Polymer 5. A gray powder, 0.53 g (42%). Anal. Calcd for $(C_{64}H_{40}S_4Si)_n$: C, 79.63; H, 4.18; S, 13.29. Found: C, 78.71; H, 4.06; S, 12.32; Br, 2.66. ^{1}H NMR (THF-d_8): δ 7.07 (dd, J = 3.2 Hz, J' = 5.2 Hz), 7.25 (d, J = 2.8 Hz), 7.30 (d, J = 2.8 Hz), 7.38 (d, J = 5.2 Hz), 7.43 (d, J = 3.2 Hz), 7.64 (s), 7.71 (d, J = 7.6 Hz), 7.76 (d, J = 7.6 Hz), 7.44−7.60 (m). ^{13}C NMR (THF-d_8): δ 126.1, 127.2, 127.5, 129.4, 130.0, 130.4, 131.6, 133.0, 133.6, 134.2, 134.5, 137.7, 139.4, 140.9, 144.6, 145.2.

Polymer 6. A brown powder, 0.46 g (42%). Anal. Calcd for $(C_{72}H_{44}S_6Si)_n$: C, 76.56; H, 3.93; S, 17.03. Found: C, 75.37; H, 3.63; S, 16.07; Br, 2.35. ^{1}H NMR (THF-d_8): δ 7.11 (dd, J = 3.2 Hz, J' = 4.4 Hz), 7.24 (d, J = 4.4 Hz), 7.27 (d, J = 3.2 Hz), 7.28−7.90 (m). ^{13}C NMR (THF-d_8): δ 123.2, 125.2, 125.9, 126.2, 127.3, 127.5, 128.6, 128.7, 129.4, 129.9, 130.0, 130.1, 130.2, 133.4, 136.4, 136.7, 137.0, 139.8, 142.5, 143.8.

Synthesis of Polymer 7 by the Grignard Coupling Polycondensation Reaction. 5,5′-Dibromo-3,3′-dihexyl-2,2′-bithiophene (1.5 g, 3.05 mmol) and Mg (0.3 g, 12.0 mmol) were dissolved in THF (50 mL). The reaction mixture was refluxed overnight. To a solution of the tetrabromo precursors **1** (1.46 g, 1.53 mmol) and [$NiCl_2$(dppp)] (30 mg) in 50 mL of THF was added the Grignard reagent in one portion. The reaction mixture was refluxed for 3 days under dry nitrogen. Upon completion, 50 mL of 1 M HCl was added. The organic layer was isolated. After removal of THF, the solid was washed with water and ethanol. The dried product was washed with acetone using a Soxhlet apparatus for 72 h to remove the catalyst residues and oligomers. The solid residue was then extracted with THF using a Soxhlet apparatus for 24 h, and the insoluble solid (cross-linked polymers) was discarded. Removal of THF gave the soluble hyperbranched polymer product. The products were dried in a vacuum oven at 120 °C for 3 days. The polymer was obtained as a yellow solid, 1.15 g (58%). Anal. Calcd for $(C_{88}H_{88}S_4Si)_n$: C, 81.18; H, 6.81; S, 9.85. Found: C, 79.98; H, 6.49; S, 9.72; Br, 1.34.^{1}H NMR ($CDCl_3$): δ 0.87 (m, 12 H), 1.23 (m, 24 H), 1.58 (m, 8 H), 2.60 (m, 8 H), 6.99 (d, J = 5.2 Hz, 4H), 7.31 (d, J = 5.2 Hz, 4H), 7.4−7.8 (m, 32 H). ^{13}C NMR ($CDCl_3$): δ 14.4, 22.9, 29.3, 29.5, 31.1, 32.0, 125.2, 126.3, 127.2, 127.6, 128.8, 129.0, 129.2, 129.9, 132.3, 133.8, 135.3, 135.9, 139.8, 142.8, 143.6, 143.9.

Polymer 8. This was prepared similar to **7**, giving a deep red solid, 1.1 g (56%). Anal. Calcd for $(C_{96}H_{92}S_6Si)_n$: C, 78.64; H, 6.32; S, 13.12. Found: C, 77.39; H, 6.16; S, 14.25; Br, 2.34.^{1}H NMR ($CDCl_3$): δ 0.92 (m, 12 H), 1.35 (m, 24 H), 1.68 (m, 8 H), 2.80 (m, 8 H), 6.80 (s, weak), 6.97−7.25 (m, 16 H), 7.35−7.70 (m, 24 H), 7.78 (d, J = 8.0 Hz, weak). ^{13}C NMR ($CDCl_3$): δ 14.4, 23.0, 29.6, 30.0, 31.0, 32.0, 124.2, 126.3, 126.5, 126.6, 126.9, 127.2, 127.6, 127.9, 128.8, 129.2, 130.4, 132.3, 133.5, 135.9, 136.4, 139.7, 140.1, 140.8, 141.0, 141.8.

Polymer 9. This was prepared similar to **7**, giving a yellow solid, 0.85 g (60%). Anal. Calcd for $(C_{140}H_{184}S_4Si)_n$: C, 83.10; H, 9.17; S, 6.34. Found: C, 83.14; H, 9.18; S, 5.78; Br, 2.59. ^{1}H NMR ($ClCD_2CD_2Cl$): δ 0.84 (br, 36 H), 1.03 (br, 24 H), 1.21 (br, 64 H), 1.60 (br, 8 H), 1.96 (br, 16 H), 2.50 (br, 8 H), 6.90−7.80 (m, 28 H). ^{13}C NMR ($CDCl_3$): δ 14.6, 23.0, 24.3, 29.7, 30.1, 30.5, 32.0, 32.3, 33.9, 40.7, 55.4, 119.6, 119.9, 121.7, 123.3, 125.4, 125.6, 126.6, 127.1, 127.3, 127.8, 129.0, 129.5, 130.1, 133.3, 133.8, 134.7, 141.3, 142.9, 143.1, 150.6, 151.3.

Ab Initio Modeling Studies. Geometry optimization calculations for two tetrahedral precursors and some model compounds were carried out using DMol^3 at the level of ab initio/DFT GGA-BLYP/DNP (quality: fine) with all electrons.[36] The energies of HOMO and LUMO, and hence the LUMO−

HOMO gaps were obtained at the optimized conformations of the molecules studied. To study the influence of torsion angles on the LUMO−HOMO gaps for the model compounds **4A′** and **D**, geometry optimizations were done with constraints on the torsion angles at certain values.

EL Device Fabrication. For the fabrication of the devices, glass substrates coated with indium−tin oxide (ITO) with a sheet resistance of 30 Ω γ^{-1} (CSG Co. Ltd.) were cleaned sequentially in ultrasonic baths of aqueous ionic detergent, acetone and anhydrous ethanol. A thin film layer of PEDOT (82 nm) and polymer **4** or **7** (80 and 100 nm, respectively) (from a 15 mg/mL solution of the polymers in THF solution) was spin-coated on the ITO surface at 800 rpm for 60 s, after which a thin layer of LiF (0.5 nm)/Ca(20 nm) was deposited on the polymer film by thermal evaporation under a vacuum of 10^{-6} Torr. The active areas of the devices were about 4.0 mm^2. The applied dc bias voltages for EL devices were in a forward direction (ITO, positive; LiF/Ca/Ag, negative). The current−voltage characteristics were measured on a voltmeter and an amperometer, respectively. The EL efficiency and brightness measurements were carried out with a calibrated silicon photodiode. All the measurements of the EL devices were carried out in air at room temperature.

Acknowledgment. We are grateful to the Agency for Science, Technology and Research (A*Star), Singapore for its financial support. We thank Ms. Li−Wei Tan and Ms. Yanqing Li for their technical assistances on PLED device fabrication.

Supporting Information Available: Figures showing ^{1}H NMR and ^{13}C NMR of **2** and **4**−**9**, MALDI−TOF MS spectrum of **2**, DSC thermogram and WAXD spectrum of **2**, and DSC and TGA thermograms of the hyperbranched polymers **4**−**9**, and text, tables, and figures discussing ab initio/DFT modeling studies on some homo- and hetero-oligothiophenes. This material is available free of charge via the Internet at http://pubs.acs.org.

References and Notes

(1) (a) Scherf, U.; List, E. *Adv. Mater.* **2002**, *14*, 477. (b) Neher, D. *Macromol. Rapid Commun.* **2001**, *22*, 1365. (c) Klärner, G.; Lee, J.-I.; Davey, M. H.; Miller, R. D. *Adv. Mater.* **1999**, *11*, 115.

(2) (a) Larmat, F.; Reynolds, J. R.; Reinhardt, B. A.; Brott, L. L.; Clarson, S. J. *J. Polym. Sci., Part A: Polym. Chem.* **1997**, *35*, 3627. (b) Blondin, P.; Bouchard, J.; Beaupré, S.; Belletête, M.; Durocher, G.; Leclerc, M. *Macromolecules* **2000**, *33*, 5874 (c) Lévesque, I.; Donat-Bouillud, A.; Tao, Y.; D'Iorio, M.; Beaupré, S.; Blondin, P.; Ranger, M.; Bouchard, J.; Leclerc, M. *Synth. Met.* **2001**, *122*, 79. (d) Charas, A.; Barbagallo, N.; Morgado, J.; Alcácer, L. *Synth. Met.* **2001**, *122*, 23. (e) Whitehead, K. S.; Grell, M.; Bradley, D. D. C.; Inbasekaran, M.; Woo, E. P. *Synth. Met.* **2000**, *111*−*112*, 181. (f) Millard, I. S. *Synth. Met.* **2000**, *111*−*112*, 119.

(3) Inbasekaran, M.; Woo, E. P.; Wu, W. S.; Bernius, M. T. PCT application W0046321A1, 2000.

(4) (a) Huang, F.; Hou, L. T.; Wu, H. B.; Wang, X. H.; Shen, H. L.; Cao, W.; Yang, W.; Cao, Y. *J. Am. Chem. Soc.* **2004**, *126*, 9845. (b) Hou, Q.; Zhou, Q.; Zhang, Y.; Yang, W.; Yang, R.; Cao, Y. *Macromolecules* **2004**, *37*, 6299. (c) Yang, J.; Jiang, C. Y.; Zhang, Y.; Yang, R. Q.; Yang, W.; Hou, Q.; Cao, Y. *Macromolecules* **2004**, *37*, 1211. (d) Huang, J.; Xu, Y. S.; Hou, Q.; Yang, W.; Yuan, M.; Cao, Y. *Macromol. Rapid Commun.* **2002**, *23*, 709. (d) Huang, J.; Niu, Y. H.; Yang, W.; Mo, Y. Q.; Yuan, M.; Cao, Y. *Macromolecules* **2002**, *35*, 6080. (e) Hou, Q.; Xu, Y. S.; Yang, W.; Yuan, M.; Peng, J. B.; Cao, Y. *J. Mater. Chem.* **2002**, *12*, 2887.

(5) (a) Jenekhe, S. A.; Osaheni, J. A. *Science* **1994**, *265*, 765. (b) Gong, X.; Iyer, P. K.; Moses, D.; Bazan, G. C.; Heeger, A. J.; Xiao, S. S. *Adv. Funct. Mater.* **2003**, *13*, 325.

(6) (a) List, E. J. W.; Günther, R.; de Frietas, P. S.; Scherf, U. *Adv. Mater.* **2002**, *14*, 374. (b) Gaal, M.; List, E. J. W.; Scherf, U. *Macromolecules* **2003**, *36*, 4236. (c) Craig, M. R.; de Kok, M. M.; Hofstraat, J. W.; Schenning, A. P. H. J.; Meijer, E. W. *J. Mater. Chem.* **2003**, *13*, 2861.

(7) (a) Setayesh, S.; Grimsdale, A. C.; Weil, T.; Enkelmann, V.; Müllen, K.; Meghdadi, F.; List, E. J. W.; Leising, G. *J. Am. Chem. Soc.* **2001**, *123*, 946. (b) Jacob, J.; Zhang, J.; Grimsdale, A. C.; Müllen, K.; Gaal, M.; List, E. J. W. *Macromolecules* **2003**, *36*, 8240. (c) Wong, K.-T.; Chien, Y.-Y.; Chen, R.-T.; Wang, C.-F.; Lin, Y.-T.; Chiang, H.-H.; Hsieh, P.-Y.; Wu, C.-C.; Chou, C.-H.; Su, Y. O.; Lee, G.-H.; Peng, S.-M. *J. Am. Chem. Soc.* **2002**, *124*, 11576. (d) Wu, C.-C.; Liu, T.-L.; Hung, W.-Y.; Lin, Y.-T.; Wong, K.-T.; Chen, R.-T.; Chen, Y.-M.; Chien, Y.-Y. *J. Am. Chem. Soc.*. **2003**, *125*, 3710.

(8) Li, Y.; Ding, J.; Day, M.; Tao, T.; Lu, J.; D'iorio, M. *Chem. Mater.* **2003**, *15*, 4936.

(9) (a) Shen, W.-J.; Dodda, R.; Wu, C.-C.; Wu, F.-I.; Liu, T.-H.; Chen, H.-H.; Chen, C.-H.; Shu, C.-F. *Chem. Mater.* **2004**, *16*, 930. (b) Pei, J.; Ni, J.; Zhou, X.-H.; Cao, X.-Y.; Lai, Y.-X. *J. Org. Chem.* **2002**, *67*, 4924. (c) Pei, J.; Ni, J.; Zhou, X.-H.; Cao, X.-Y.; Lai, Y.-X. *J. Org. Chem.* **2002**, *67*, 8104. (d) Wu, R.; Schumm, J. S.; Pearson, D. L.; Tour, J. M. *J. Org. Chem.* **1996**, *61*, 6906. (e) Tour, J. M.; Wu, R.; Schumm, J. S. *J. Am. Chem. Soc.* **1990**, *112*, 5662. (f) Wu, C.-C.; Lin, Y.-T.; Wong, K.-T.; Chen, R.-T.; Chien, Y.-Y. *Adv. Mater.* **2004**, *16*, 61.

(10) Pei, J.; Wang, J.-L.; Cao, X.-Y.; Zhou, X.-H.; Zhang, W.-B. *J. Am. Chem. Soc.* **2003**, *125*, 9944.

(11) Xia, C.; Advincula, R. C. *Macromolecules* **2001**, *34*, 6922.

(12) (a) Xu, M. H.; Zhang, H. C.; Pu, L. *Macromolecules* **2003**, *36*, 2689. (b) He, Q. G.; Bai, F. L.; Yang, J. L.; Lin, H. Z.; Huang, H. M.; Yu, G.; Li, Y. F. *Thin Solid Films* **2002**, *417*, 183. (c) Jikei, M.; Mori, R.; Kawauchi, S.; Kakimoto, M.; Taniguchi, Y. *Polym. J.* **2002**, *34*, 550. (d) Yao, J. Z.; Son, D. Y. *Organometallics* **1999**, *18*, 1736.

(13) Wang, S.; Oldham, W. J.; Hudack, R. A.; Bazan, G. C. *J. Am. Chem. Soc.* **2000**, *122*, 5695.

(14) (a) Sengupta, S.; Muhuri, S. *Tetrahedron Lett.* **2004**, *45*, 2895. (b) Sengupta, S.; Sadhukhan, S. K. Muhuri, S. *Synlett* **2003**, 2329. (c) Sengupta, S.; Sadhukhan, S. K. *Tetrahedron Lett.* **1998**, *39*, 1237. (d) Sengupta, S.; Sadhukhan, S. K. *Tetrahedron Lett.* **1999**, *40*, 9157. (e) Sengupta, S.; Sadhukhan, S. K. *Organometallics* **2001**, *20*, 1889. (f) Sengupta, S.; Purkayastha, P. *Org. Biomol. Chem.* **2003**, *1*, 436. (g) Lambert, C.; Gaschler, W.; Nöll, G.; Weber, M.; Schmälzlin, E.; Bräuchle, C.; Meerholz, K. *J. Chem. Soc., Perkin Trans. 2* **2001**, 964. (h) Zhao, H.; Tanjutco, C.; Thayumanavan, S. *Tetrahedron Lett.* **2001**, *42*, 4421. (j) Robinson, M. R.; Wang, S.; Bazan, G. C.; Cao, Y. *Adv. Mater.* **2000**, *12*, 1701. (i) Armaroli, N.; Balzani, V.; Collin, J.-P.; Gavińa, P.; Sauvage, J.-P.; Ventura, B. *J. Am. Chem. Soc.* **1999**, *121*, 4397.

(15) (a) Laliberte, D.; Maris, T.; Wuest, J. D. *Can. J. Chem.* **2004**, *82*, 386. (b) Fournier, J. H.; Wang, X.; Wuest, J. D. *Can. J. Chem.* **2004**, *81*, 376. (c) Fournier, J. H.; Maris, T.; Wuest, J. D.; Guo, W. Z. Galoppini, E. *J. Am. Chem. Soc.* **2003**, *125*, 1002. (d) Kaminorz, Y.; Schulz, B.; Schrader, S.; Brehmer, L. *Synth. Met.* **2001**, *122*, 115.

(16) (a) Chan, L.-H.; Lee, R.-H.; Hsieh, C.-F.; Yeh, H.-C.; Chen, C.-T. *J. Am. Chem. Soc.* **2002**, *124*, 6469. (b) Chan, L.-H.; Yeh, H.-C.; Chen, C.-T. *Adv. Mater.* **2001**, *13*, 1637. (c) Yeh, H.-C.; Lee, R.-H.; Chan, L.-H.; Lin, T.-Y. J.; Chen, C.-T.; Balasubramaniam, E.; Tao, Y.-T. *Chem. Mater.* **2001**, *13*, 2788.

(17) (a) Rathore, R.; Burns, C. L.; Deselnicu, M. I. *Org. Lett.* **2001**, *3*, 2887. (b) Zimmermann, T. J.; Freundel, O.; Gompper, R.; Müller, T. J. J. *Eur. J. Org. Chem.* **2000**, 3305.

(18) Li, Q.; Rukavishnikov, A. V.; Petukhov, P. A.; Zaikova, T. O.; Keana, J. F. W. *Org. Lett.* **2002**, *4*, 3631.

(19) Oldham, W. J., Jr.; Lachicotte, R. J.; Bazan, G. C. *J. Am. Chem. Soc.* **1998**, *120*, 2987−2988.

(20) (a) Liu, X.-M.; He, C.; Xu, J.-W. *Tetrahedron Lett.* **2004**, *45*, 1593. (b) Liu, X.-M.; Xu, J.-M.; He, C. *Tetrahedron Lett.* **2004**, *45*, 1507. (c) Liu, X.-M.; He, C.; Huang, J.-C. *Tetrahedron Lett.* **2004**, *45*, 6173. (d) Liu, X.-M.; He, C.; Huang, J.; Xu, J. *Chem. Mater.* **2005**, *17*, 434. (e) He, C.; Xiao, Y.; Huang, J.; Lin, T.; Mya, K. Y.; Zhang, X. *J. Am. Chem. Soc.* **2004**, *126*, 7792.

(21) Liu, X.-M.; He, C.; Hao, X.-T.; Tan, L.-W.; Li, Y.; Ong, K. S. *Macromolecules* **2004**, *37*, 5965.

(22) Inoue, K. *Prog. Polym. Sci.* **2000**, *25*, 453.

(23) Jikei, M.; Kakimoto, M.-A. *Prog. Polym. Sci.* **2001**, *26*, 1233.

(24) (a) Wang, F.; Kalai, B. R.; Neckers, D. C. *Macromolecules* **2003**, *36*, 8225. (b) Chen, J. W.; Peng, H.; Law, C. C. W.; Dong, Y. P.; Lam, J. W. Y.; Williams, I. D.; Tang, B. Z. *Macromolecules* **2003**, *36*, 4319. (c) Sun, Q. H.; Xu, K. T.; Peng, H.; Zheng, R. H.; Haussler, M.; Tang, B. Z. *Macromolecules* **2003**, *36*, 2309. (d) Chen, J. W.; Law, C. C. W.; Lam, J. W. Y.; Dong, Y. P.; Lo, S. M. F.; Williams, I. D.; Zhu, D. B.; Tang, B. Z. *Chem. Mater.* **2003**, *15*, 1535. (e) Chen, J. W.;

Xie, Z. L.; Lam, J. W. Y.; Law, C. C. W.; Tang, B. Z. *Macromolecules* **2003**, *36*, 1108.
(25) Kim, Y. H.; Webster, O. W. *J. Am. Chem. Soc.* **1990**, *112*, 4592.
(26) Kagan, J.; Arora, S. K. *Tetrahedron Lett.* **1983**, *24*, 4043.
(27) (a) O'Brien, D. F.; Burrows, P. E.; Forrest, S. R.; Konne, B. E.; Loy, D. E.; Thompson, M. E. *Adv. Mater.* **1998**, *10*, 1108. (b) Koene, B. E.; Loy, D. E.; Thompson, M. E. *Chem. Mater.* **1998**, *10*, 2235.
(28) Sengupta, S.; Sadhukhan, S. K.; Muhuri, S. *Tetrahedron Lett.* **2002**, *43*, 3521.
(29) (a) Jo, J.; Chi, C.; Höger, S.; Wegner, G.; Yoon, D. Y. *Chem.—Eur. J.* **2004**, *10*, 2681. (b) Li, Y. N.; Ding, J. F.; Day, M.; Tao, Y.; Lu, J. P.; D'iorio, M. *Chem. Mater.* **2004**, *16*, 2165. (c) Lee, S. H.; Tsutsui, T. *Thin Solid Films* **2000**, *363*, 76.
(30) Meng, H.; Zheng, J.; Lovinger, A. J.; Wang, B.-C.; Patten, P. G. V.; Bao, Z. *Chem. Mater.* **2003**, *15*, 1778.
(31) Roncali, J. *Chem. Rev.* **1992**, *92*, 711.
(32) (a) Bongini, A.; Bottoni, A. *J. Phys. Chem. A* **1999**, *103*, 6800. (b) Breza, M.; Lukeš, V.; Vrăbel, I. *Theor. Chem.* **2001**, *572*, 151.
(33) Peng, Q.; Lu, Z.-Y.; Huang, Y.; Xie, M.-G.; Xiao, D.; Han, S.-H.; Peng, J.-B.; Cao, Y. *J. Mater. Chem.* **2004**, *14*, 396.
(34) (a) Yu, W.-L.; Pei, J.; Cao, Y.; Huang, W.; Heeger, A. J. *Chem. Commun.* **1999**, 1837. (b) Schoo, H. F. M.; Demandt, R. C. J. E.; Vleggaar, J. J. M.; Liedenbaum, C. T. H. *Macromol. Symp.* **1997**, *125*, 165.
(35) (a) Musick, K. Y.; Hu, Q.-S.; Pu, L. *Maromolecules* **1998**, *31*, 2933. (b) Jones, C. L.; Higgins, S. J. *J. Mater. Chem.* **1999**, *9*, 865.
(36) (a) Delley, B. *J. Chem. Phys.* **1990**, *92*, 508. (b) Delley, B. *J. Chem. Phys.* **2000**, *113*, 7756.

MA047686Q